CERN-PBC-REPORT-2024-001

26 June 2024
vera.cilento@cern.ch

Vertical Spin build-up due to Vertical Offset in Quadrupoles and Horizontal Betatron Oscillations

V. Cilento, C. Carli
CERN, CH-1211 Geneva, Switzerland

Keywords: cpEDM, frozen spin, hybrid ring, spin precession, electric focusing

Summary

Many proposals to measure a possible small Electric Dipole Moment (EDM) of charged particles are based on the magic energy concept. Without EDM and for a ring without imperfections, an initial longitudinal polarization of a bunch is maintained in electro-static bendings by operation at a particular energy called the magic energy. A finite EDM generates a spin rotation into the vertical direction. The initial proposal foresaw focusing with electro-static quadrupolar components, whereas the hybrid ring uses magnetic quadrupoles. This study investigates the vertical spin build-up in magic energy charged particle (cpEDM) rings caused by imperfections, focusing on the effects caused by vertical offsets in both magnetic and electric quadrupoles and their interplay with horizontal betatron oscillations. Through a comprehensive analysis that compares analytical estimates with simulation models, the research highlights discrepancies between the results.

Contents

1 Introduction

In the pursuit of measuring the Electric Dipole Moment (EDM) of charged particles in storage rings, numerous experimental approaches are being explored. Typically, charged particle EDM rings are operated at the "frozen spin" condition, such without EDM an initial longitudinal polarization of a bunch at injection is maintained. This condition requires that, in absence of an EDM and with the well known Magnetic Dipole Moment (MDM) in a perfect machine, bunches with initial longitudinal polarization (parallel or antiparallel to the direction of movement) remain longitudinally polarized. This implies that the spin of a reference particle (reference energy and reference orbit in perfect machine) rotates together with the direction of the trajectory. This is achieved by an appropriate choice of the electric and magnetic fields of bending elements [1, 2, 3, 4, 5, 6]. The effect of a finite EDM is a rotation of the spin around a radial direction from the longitudinal direction into the vertical direction. In an EDM ring, the resulting vertical spin build up, which is very small for the smallest EDM to be detected in typical proposals, is measured with a polarimeter. A special case underlying the study presented here and possible only for particles with positive anomalous magnetic moment $G > 0$ as for example protons, is operation with beams at the "magic energy", where the "frozen spin" condition is met with electro-static bendings [7].

Systematic effects, i.e. spin rotations into vertical direction not related to a finite EDM, pose a significant challenge in these measurements. They may arise from various sources, including imperfections in the focusing structure, external magnetic fields, or even gravitational effects. These effects generate spin rotations as the ones due an EDM and can obscure or mimic the signals attributed to an EDM, thus impacting the sensitivity and accuracy of the experiments [8].

This paper delves into a specific systematic effect: the combination of the vertical offset between the beam and a quadrupole and horizontal betatron oscillations, as depicted in Figure 1. For simulations, the symmetric hybrid ring lattice setup [9] is used to investigate this effect in both electro-static and hybrid EDM rings.

Simulations and analytical estimates are used to assess the magnitude of this effect and its potential as a source of systematic error in the context of achieving the target sensitivity for EDM measurements. These elements conjointly introduce complex spin rotations around both longitudinal and vertical axes, culminating in a classical geometric phase effect.

2 Description of the effect

The reasoning motivating the study is a classical geometric phase effect depicted in Figure 1. In case of a magic energy hybrid ring (electro-static bendings and magnetic quadrupoles), the spin rotates faster than the particle direction inside the magnetic quadrupoles. For the trajectory with positive horizontal position x shown through an QF quadrupole, the radial spin component is positive at the entrance and negative at the exit. A vertical offset of the beam with respect to the quadrupole center generates longitudinal magnetic field components with opposite sign for the magnet entrance and exit fringe field. The resulting small changes of the vertical spin component add up.

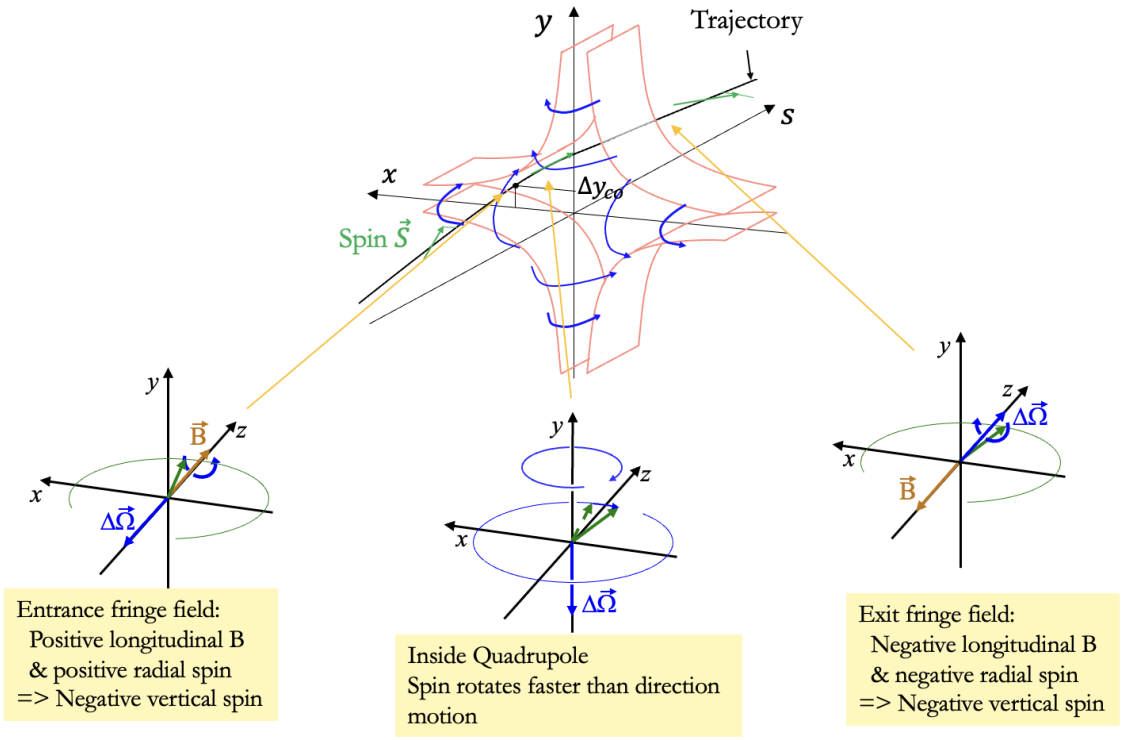

Figure 1: Detailed description of the mechanism of the geometric phase effect described in this paper.

2.1 Thomas-BMT Equation to describe the rotation of the particle spin

Spin rotations of charged particles with both a magnetic dipole moment (MDM) and an electric dipole moment (EDM) aligned with the particle spin are described by the Thomas-BMT equation with additional terms due to the EDM. The vector $\vec{S}$ is a unit vector describing the direction of the spin in the inertial rest frame of the particle. The time derivative of the spin direction $\vec{S}$ of a particle with charge q and mass m in a magnetic field $\vec{B}$ and an electric field $\vec{E}$ defined in the laboratory frame is given by [10, 11]:

$$
\begin{aligned}
\frac{d\vec{S}}{dt} &= \vec{\omega}_s \times \vec{S} \\
\vec{\omega}_s &= \vec{\omega}_{\mathrm{MDM}} + \vec{\omega}_{\mathrm{EDM}} \\
&= -\frac{q}{m}\left[\left(G+\frac{1}{\gamma}\right)\vec{B} - G\frac{\gamma-1}{\gamma}\frac{\vec{B}\cdot\vec{\beta}}{\beta^2}\vec{\beta} - \left(G+\frac{1}{\gamma+1}\right)\vec{\beta}\times\frac{\vec{E}}{c}\right. \\
&\quad \left. + \frac{\eta}{2}\left(\frac{\vec{E}}{c} - \frac{\gamma-1}{c\gamma}\frac{\vec{E}\cdot\vec{\beta}}{\beta^2}\vec{\beta} + \vec{\beta}\times\vec{B}\right)\right] \\
&= -\frac{q}{m}\left[\left(G+\frac{1}{\gamma}\right)\vec{B}_\perp + (G+1)\frac{\vec{B}_\parallel}{\gamma} - \left(G+\frac{1}{\gamma+1}\right)\vec{\beta}\times\frac{\vec{E}}{c}\right. \\
&\quad \left. + \frac{\eta}{2}\left(\frac{\vec{E}_\perp}{c} + \frac{1}{\gamma}\frac{\vec{E}_\parallel}{c} + \vec{\beta}\times\vec{B}\right)\right] \qquad (1)
\end{aligned}
$$

where β and γ are the relativistic factors and $\vec{\beta} = \frac{\vec{v}}{c}$ is a vector with length β and a direction parallel to the velocity ($\vec{v}$ and c are the velocity of the particle and the velocity of light, respectively). The quantities G and η describe the well-known magnetic moment and the EDM to be measured, respectively. For the case of protons $G = 1.79285$. Note that for a proton EDM of $d_s = 10^{-29}\, e\, cm$, which is often quoted as the expected sensitivity of the currently proposed experiments, η is as low as $\eta_s = 1.9 \times 10^{-15}$. The indices $\parallel$ and $\perp$ denote the component of a vector parallel and perpendicular to the direction of movement; for example, for the electric field $\vec{E}_\parallel = (\vec{t}\cdot\vec{E})\vec{t}$ and $\vec{E}_\perp = \vec{E} - (\vec{t}\cdot\vec{E})\vec{t}$ where $\vec{t} = \vec{\beta}/\beta = \vec{p}/p$ is a unit vector pointing in the direction of the movement. $\vec{p} = \gamma m\vec{\beta}$ is the momentum vector and p is the absolute value of the momentum.

2.2 Analytical Estimates for the magnetic case

As a first step of a quantitative estimate of the effect, the radial spin components at the location of the fringe fields has to be estimated. From the Thomas-BMT equation (see Eq. 1) and the equations of motion, one obtains the vertical components of the angular frequencies describing the rotation of the spin and the momentum, the spin rotation $\omega_{s,y}$ and rotation of particle direction $\omega_{p,y}$ are given by the following relations:

$$
\omega_{s,y} = -\frac{q}{m}\left(G+\frac{1}{\gamma}\right)B_y \quad \text{and} \quad \omega_{p,y} = -\frac{q}{m\gamma}B_y. \qquad (2)
$$

Based on the ratio between these two angular frequencies, the radial component of the spin is estimated as:

$$
S_x \approx (\omega_{s,y}/\omega_{p,y})x' = (\gamma G+1)x' \quad \text{and} \quad S_x - x' \approx \gamma G x'. \qquad (3)
$$

This relation would be exact for magnetic focusing only. With part of the focusing generated by the electrostatic bendings, this relation is still valid at least as an order of magnitude estimate. The integrated longitudinal field through the fringe field of a magnetic

quadrupole from outside the fringe field to inside the magnet with focusing strength k at the position of the trajectory is given by:

$$\int B_s ds = \pm \frac{m\gamma\beta c}{q} kx\Delta y_{co} \tag{4}$$

with the upper (lower) sign for the entrance (exit). This generates rotation around the longitudinal axis of:

$$\Delta\alpha_s = -\frac{q}{m}\frac{G+1}{\gamma}\int B_s \frac{ds}{\beta c} = \pm(G+1)kx\Delta y_{co} \tag{5}$$

and gives a vertical spin component of:

$$\Delta S_y = \Delta\alpha_s(S_x - x') = \pm(G+1)k\Delta y_{co}x(S_x - x') \approx \pm\gamma G(G+1)k\Delta y_{co}xx'. \tag{6}$$

Averaging xx' over the betatron oscillations with β_x and α_x the Twiss parameters and J_x the action variable, we get:

$$\langle xx' \rangle = \frac{1}{2\pi}\int d\mu \sqrt{2J_x/\beta_x}\,\cos\mu\,\sqrt{2J_x/\beta_x}\,(\sin\mu - \alpha_x\cos\mu) = -J_x\alpha_x. \tag{7}$$

Adding the contributions from the quadrupole entrance (index i) and exit (index o) and dividing by the revolution period, one obtains an estimate for the vertical spin build up rate:

$$\dot{S}_y = \frac{\gamma G(G+1)k}{C/(\beta c)}(\Delta y_{co,i}\alpha_{x,i} - \Delta y_{co,o}\alpha_{x,o})J_x. \tag{8}$$

This is expected to be an upper limit for the hybrid ring and should be exact for structures without bendings.

3 Simulation Results

The symmetric-hybrid ring lattice design [9] was employed to simulate the effects of a vertical offset in the quadrupole focusing elements. Specifically, for the first simulation, a single QF quadrupole with an intentional misalignment was considered to determine its impact on the spin dynamics of a circulating beam. In particular, the special simple case chosen for the simulation is depicted in Figure 2. One magnetic quadrupole is vertically misaligned and two magnetic correctors before and after are used to correct the vertical closed orbit distortion in the rest of the ring. Thus, only the region around the misaligned quadrupole contributes to spin rotations into the vertical plane by the effect described and analytical estimated can be evaluated easily.

Spin tracking results were obtained with BMAD [12] for a longitudinally polarized beam.

The computational analysis was extended to particles undergoing different betatron oscillations, providing a comprehensive view of the spin behavior under varied conditions. The results of these simulations were juxtaposed with analytical estimates, facilitating a robust comparison and enhancing the understanding of systematic effects in the simulation setup.

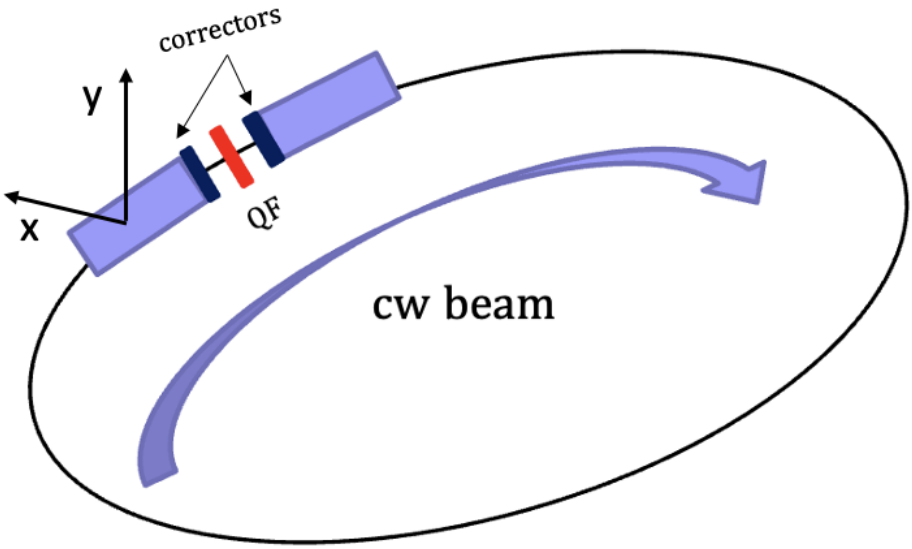

Figure 2: Sketch of the simulation set-up with one vertically misaligned quadrupole and correctors before and after to correct the vertical orbit distortions in the rest of the ring.

3.1 Effect in a Focusing Quadrupole

Simulation results are presented for two cases, considering the effect of a vertical offset in one of the quadrupole focusing elements (QF). The offset introduces variations in spin dynamics over time for particles executing different betatron oscillations, namely betatron 1 (phase, μ=0°), 2 (μ=120°) and 3 (μ=240°) and for different values of the action variable J_x. The value of the ϵ_{rms} is 0.214 μm.

3.1.1 Simulation Results

For the first scenario, an offset of 0.1 mm was introduced. The spin tracking results, displayed in Figure 3, illustrate the vertical and horizontal spin variations for a longitudinally polarized beam under different betatron oscillations. It was observed that the vertical spin component exhibited as expected a systematic trend over time, with the magnitude of the spin deviation proportional to the amplitude of the betatron oscillation and independent of the actual variable, J_x (see that the curves for the cases with the same J_x overlap).

The second case involved an offset of 0.2 mm. As shown in Figure 4, this factor two greater offset led to an increase of the vertical spin build-up by as well a factor two.

For completeness, the time evolution of the horizontal spin component is shown as well, but not relevant for the initial vertical spin build-up. One notes that the observed initial horizontal spin build-up is independent of the vertical quadrupole offset and approximately proportional to the horizontal action variable. An hypothesis explaining this observation and horizontal spin rotations with opposite sign observed with electric quadrupoles is given at the end of this report (see Section 5).

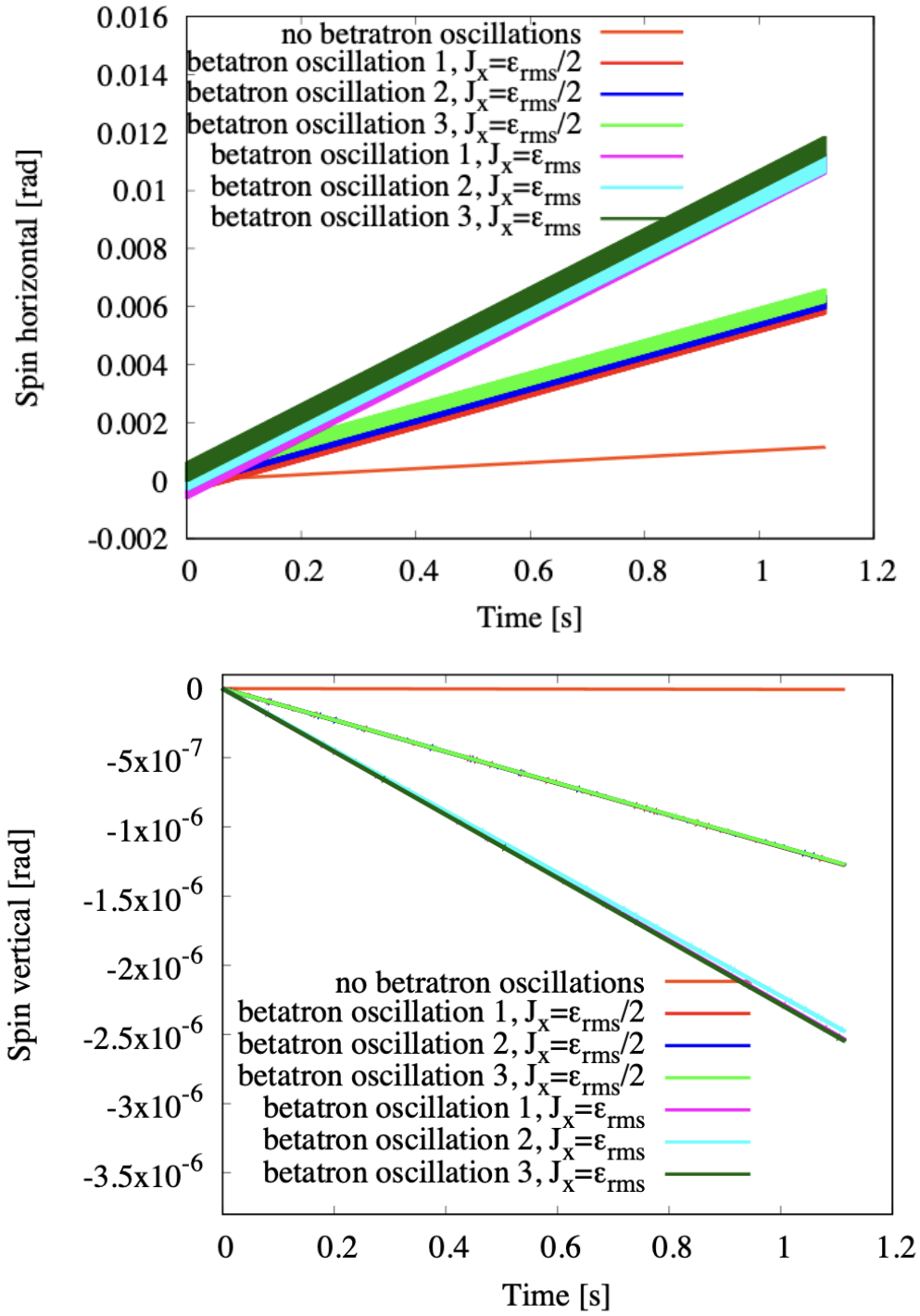

Figure 3: Horizontal and vertical spin build-up for different betatron oscillations phases and different values of the action variable J_x. Case of magnetic QF offset of 0.1 mm.

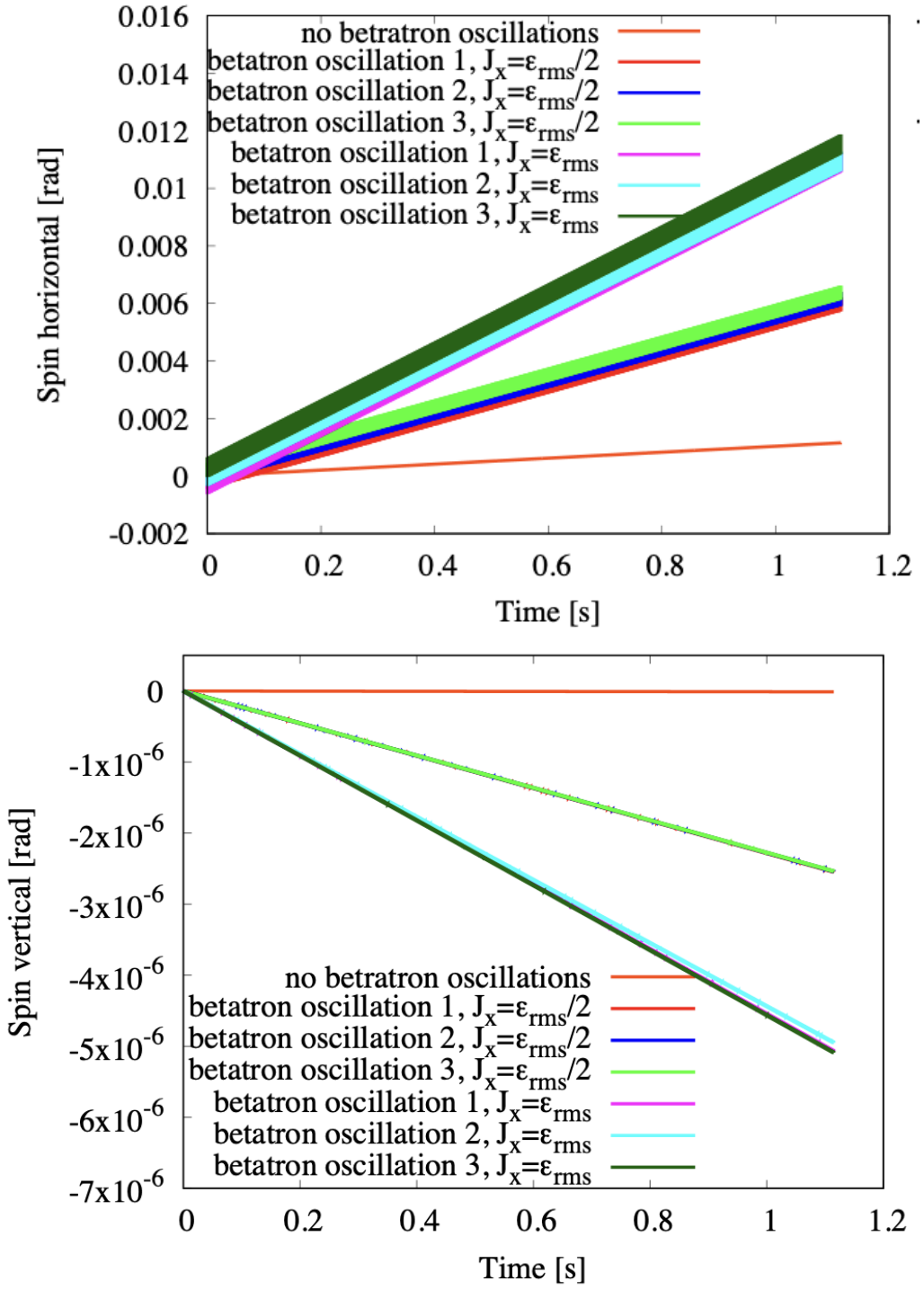

Figure 4: Horizontal and vertical spin build-up for different betatron oscillations phases and different values of the action variable J_x. Case of magnetic QF offset of 0.2 mm.

3.1.2 Comparison Between Analytical Estimates and Simulation Results

The analytical and simulation results were rigorously compared to assess the consistency of the spin dynamics predictions. For an offset of 0.1 mm, the analytical estimates yielded a vertical spin build-up rate of $\dot{S}_y = 5.9 \cdot 10^{-6}$ rad/s for a beam emittance $\epsilon_{rms} = 0.214$ μm. Simulations for the structure with bendings presented differing results as depicted in Figure 3. Here, two scenarios were analyzed: one with an offset halving the emittance, and another matching the emittance, resulting in $\dot{S}_y$ values of $-1.28 \cdot 10^{-6}$ rad/s and $-2.54 \cdot 10^{-6}$ rad/s, respectively.

A similar comparative analysis was carried out for a larger offset of 0.2 mm. The simulations, as shown in Figure 4, indicated a more pronounced effect on the spin build-up rate, as expected, with values twice as large as those observed in the 0.1 mm offset case.

For a structure without bendings, instead, simulations were also carried out in order to asses if there was good agreement between analytical estimates and simulation results. The offset considered has been 0.1 mm and the values obtained have been $\dot{S}_y$ of $-1.51 \cdot 10^{-6}$ rad/s for the half emittance and $-3.02 \cdot 10^{-6}$ rad/s for the rms emittance, respectively. This result shows an important discrepancy between analytical estimates and simulation results also for this case. In conclusion, the effect seen in simulations is about -1/2 times the one from the estimate.

A possible reason for the discrepancy between simulation results and estimates is that Eq. 3 is expected to be valid only approximately. To verify this hypothesis, the quantity $(S_x - x') * x$ is plotted in Figure 5. From the analytical estimates we have $\langle (S_x - x') * x \rangle$ approximately equal to $-5.39 \cdot 10^{-7}$ rad m. The simulation results for different betatron oscillations, in Figure 5), are in close agreement with these analytical estimates. In particular, we got for betatron 1 a $\langle (S_x - x') * x \rangle$ value of $5.41 \cdot 10^{-7}$ rad m at the quadrupole entrance and $-5.42 \cdot 10^{-7}$ rad m at the quadrupole exit, for betatron 2 a $\langle (S_x - x') * x \rangle$ value of $\pm 5.28 \cdot 10^{-7}$ rad m at the quadrupole entrance and exit, for betatron 3 a $\langle (S_x - x') * x \rangle$ value of $5.41 \cdot 10^{-7}$ rad m at the quadrupole entrance and $-5.46 \cdot 10^{-7}$ rad m at the quadrupole exit. These results are giving us a very important insight that the main discrepancies are not coming for sure from the value $\langle (S_x - x') * x \rangle$ and so the source of the discrepancy should be some other mechanism still to be understood.

3.2 Effect in a Defocusing Quadrupole

Also for this case, the lattice design of the symmetric-hybrid ring was adapted [9] to incorporate a vertical offset in one QD quadrupole. This adjustment, complemented by the addition of magnetic correctors, was implemented to study the resulting spin dynamics without inducing orbit distortions.

3.3 Simulation Results

Spin tracking simulations were conducted for a longitudinally polarized beam, with the results computed for particles undergoing different betatron oscillations. The impact of the QD offset in comparison with the impact of the QF offset on spin dynamics is visually represented in Figure 6, which illustrates the change in spin vertical and horizontal components over

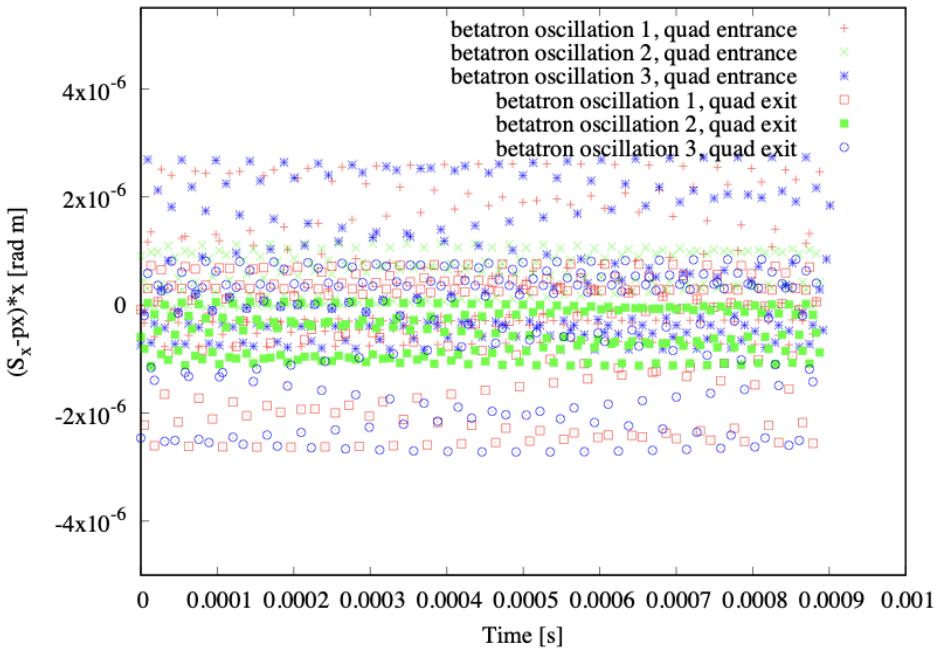

Figure 5: $(S_x - x') * x$ over time at the quadrupole (magnetic QF) entrance and exit for different betatron ocillascions.

time. From the figure it is possible to see that the impact of the QD is smaller since it has a smaller α and so a smaller beam size in comparison to the QF quadrupole. The results are behaving exactly as expected.

4 Lattice with Electric Focusing

Prompted by internal discussions [13], this study investigates the effect of horizontal betatron oscillations and vertical offsets of electro-static quadrupoles. The simulation set-up using the lattice of the hybrid ring with the magnetic quads replaced by electro-static ones is anyhow described later.

4.1 Analytical Estimates

To quantify the initial expectations of the effects, analytical estimates were developed to assess the impact of electric quadrupoles on particle spin dynamics. The electric field $\vec{E}$ and potential U within the quadrupole are represented as (see Figure 7):

$$\vec{E} = k\frac{\beta^2 mc^2}{q}(-x, y) \quad \text{and} \quad U = k\frac{\gamma\beta^2 mc^2}{q}\frac{x^2 - y^2}{2}. \tag{9}$$

These lead to a change in the Lorentz factor of:

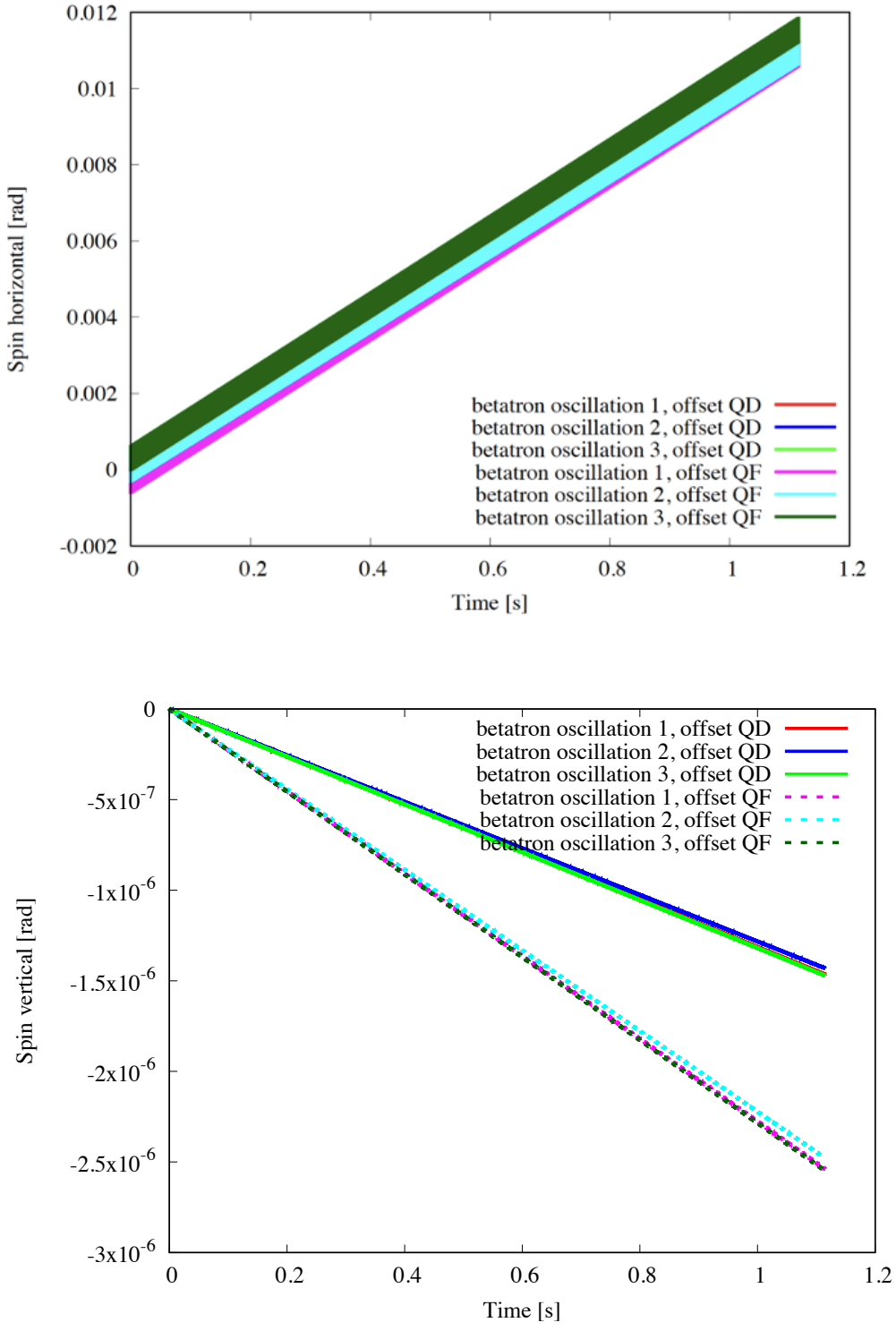

Figure 6: Horizontal and vertical spin build-up for different betatron oscillations for the magnetic QD offset of 0.1 mm and comparison with the QF case.

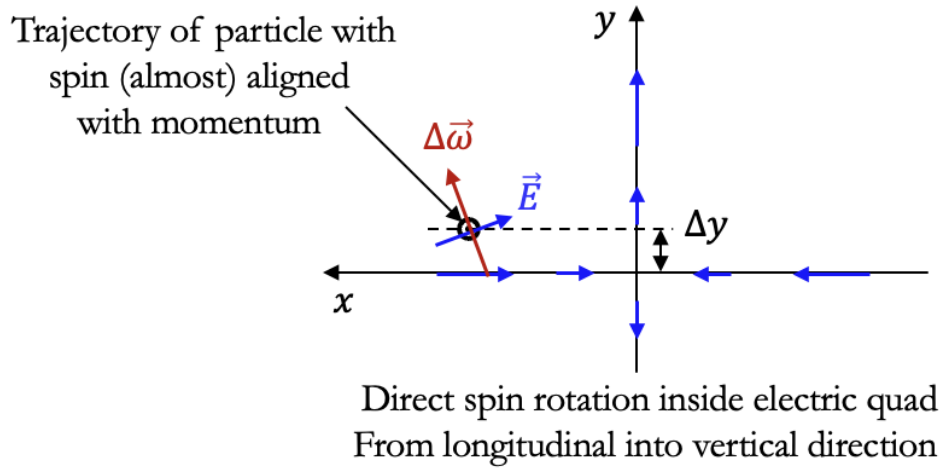

Figure 7: Sketch to describe the spin rotation in the electric quadrupole.

$$\Delta\gamma = -\frac{qU}{mc^2} = k\gamma\beta^2\frac{y^2 - x^2}{2}, \tag{10}$$

which implies that the particle kinetic energy is not the magic energy any more. Thus, the angular frequencies describing the rotation of the spin given in Eq. 1 and the one describing the particle direction $\vec{\omega}_p = \frac{q}{m\gamma\beta^2}\vec{\beta} \times \frac{\vec{E}}{c}$ are not the same any more, resulting in an average vertical spin build-up of a particle with (initial) longitudinal polarization. The difference between the angular frequencies is given by:

$$\Delta\omega = \omega_s - \omega_p = \frac{q}{m}\left[\left(G + \frac{1}{\gamma+1}\right) - \frac{1}{\gamma\beta^2}\right]\vec{\beta} \times \frac{\vec{E}}{c} = \frac{q}{m}\left(G - \frac{1}{\gamma^2-1}\right)\vec{\beta} \times \frac{\vec{E}}{c}. \tag{11}$$

The radial component of this difference of angular frequencies describing the rotation from the initial longitudinal spin into the vertical direction is given by:

$$\Delta\omega_x = -\frac{q}{m}\left(G - \frac{1}{\gamma^2-1}\right)\frac{\beta E_y}{c} = -\frac{\beta c k^2}{\gamma}(\Delta y^2 - x^2)\Delta y \approx \frac{\beta c}{\gamma}k^2x^2\Delta y. \tag{12}$$

Skipping the higher-order terms proportional to Δy^3 and averaging over the circumference $\frac{L_{quad}}{C}$ and replacing x^2 by $< x^2 >= \beta_x J_x$ yield a spin build-up rate $\dot{S}_y$ for an initial polarization parallel to the movement of:

$$\dot{S}_y = -\Delta\hat{\omega}_x = -\frac{L_{quad}\beta c k^2 \beta_x J_x \Delta y}{C\gamma}. \tag{13}$$

For a quadrupole length $L_{quad} = 0.4$ m, circumference $C = 800$ m, and given values of k, β_x, and J_x, the analytical estimation of the spin build-up rate $\dot{S}_y$ is found to be 0.757μrad/s for $\Delta y = -0.1$ mm, which shows good agreement with the simulated value, that gives $\dot{S}_y = 0.788\mu$rad/s (see Section 4.2).

4.2 Simulation Results

Simulations were executed for offsets of 0.1 mm and 0.2 mm in the QF quadrupole to investigate the spin precession rates for particles performing various betatron oscillations.

For an offset of 0.1 mm, the spin tracking outcomes for both electric and magnetic quadrupoles are illustrated in Figure 8. In particular, we can see that the vertical spin build up in the case of the electric quadrupoles decreased by a factor close to 3 and it has a difference in sign with respect to magnetic quadrupoles. An increased offset of 0.2 mm amplifies the observed effects, as depicted in Figure 9. In particular, we can see as expected that the effect is proportional to the quadrupole offset, as in the magnetic case.

Moreover, observation on horizontal spin drifts due to betatron oscillations with magnetic and electric focusing lead to different sign for electric and magnetic focusing. The possible qualitative hypothetical explanation is explained in Section 5.

5 Interpretation of the observed spin rotation in the horizontal plane

A build-up of a horizontal spin component independent of the vertical quadrupole offset and about proportional to the horizontal action variable has been observed in the simulations. For the cases simulated, i.e., a clockwise beam and initial polarization parallel to the particle direction, the sign of this horizontal spin build-up rate is positive for the hybrid ring with magnetic focusing and negative for electric focusing. The qualitative explanation give here is valid for the case without RF system as simulated in this report. The horizontal betatron oscillations increase the particle path and, thus, the traversal time through the electro-static bending element increasing the deflection. Note that similar phenomena are expected as a function of the vertical action variable.

The increase of the deflection inside bendings leads, in average, to a displacement of the trajectory to the interior of the ring such that the kinetic energy of the particle is increased inside the electrostatic bends and shifted to slightly above magic energy. Thus, inside bending elements the spin rotates faster than the momentum leading to a build-up of a negative horizontal spin components about proportional to the action variable. Note that the change in kinetic energy inside the electrostatic quadrupoles bending the beam in average towards the outside is small such that the rotations of the spin w.r.t. the direction give only small additional contributions. In case of magnetic quadrupoles, their additional contribution has to be taken into account. The magnetic quadrupoles have to compensate the average additional deflection in bendings towards the inside. The rotation of the spin in magnetic fields is faster than the rotation of the momentum. This leads to an additional positive horizontal spin build-up dominating over the one inside bendings and about proportional to the action variable.

Additional phenomena have to be taken onto account if an RF system as needed for a cpEDM measurement ring is present. The change of the average revolution time per turn (due to the change of the path per turn and the change of the kinetic energy and, thus, velocity inside bendings) is compensated by a small change of the average particle energy such that average revolution time is independent from the action variable. Finally, particles

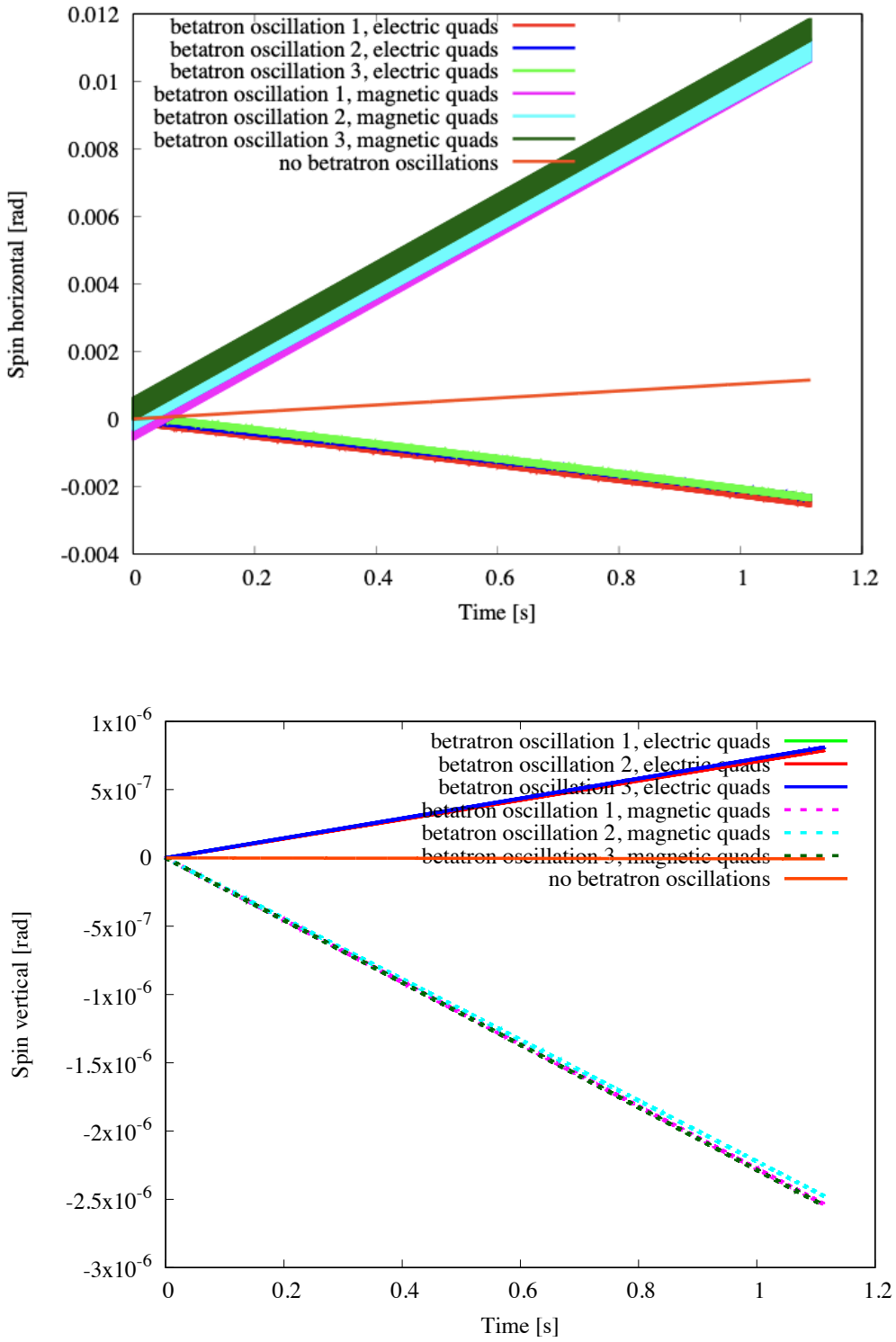

Figure 8: Horizontal and vertical spin build-up for different betatron oscillascions phases for the electric QF offset of 0.1 mm and comparison with the magnetic case.

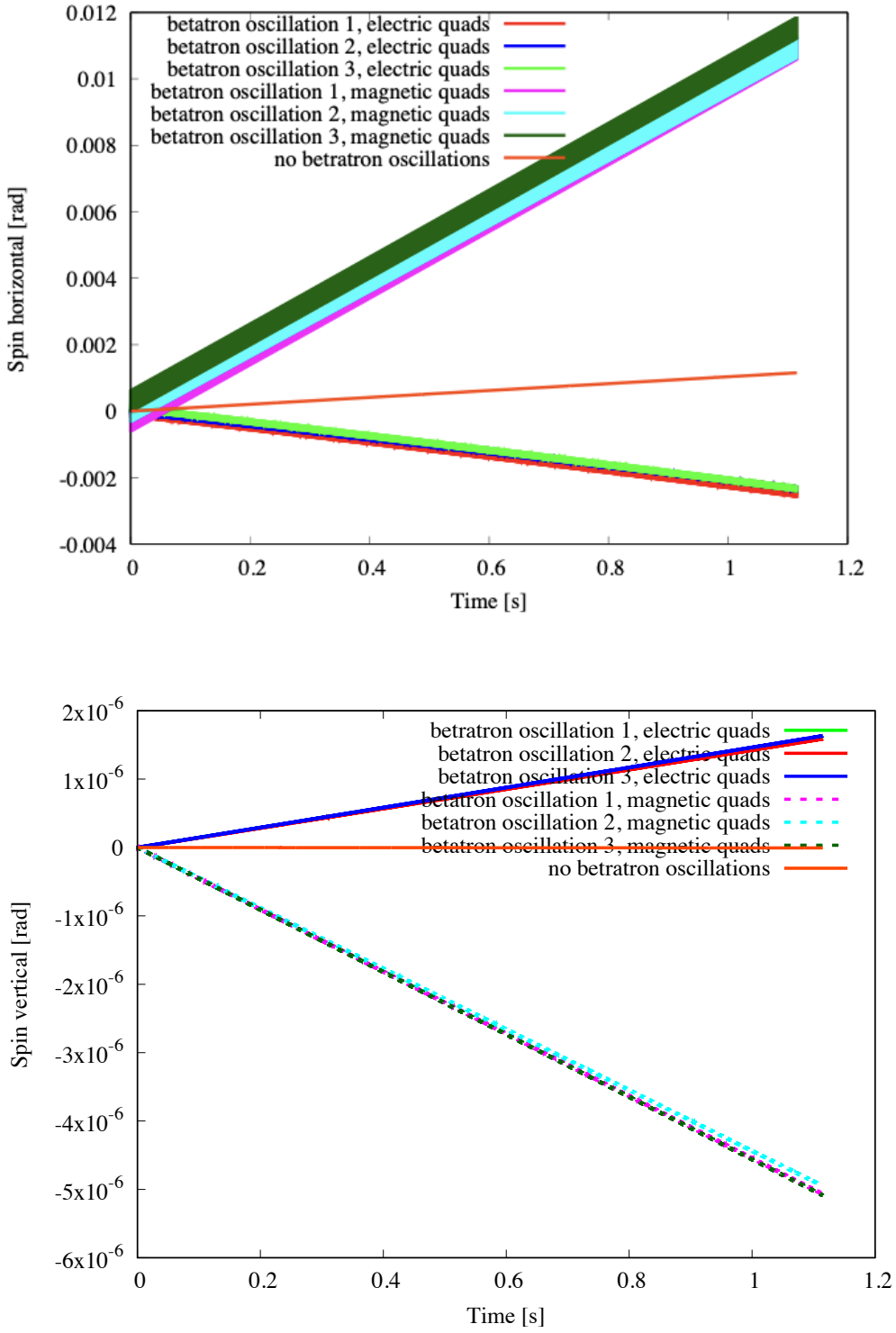

Figure 9: Horizontal and vertical spin build-up for different betatron oscillascions phases for the electric QF offset of 0.2 mm and comparison with the magnetic case.

with different action variables will have different spin rotations w.r.t. the particle direction leading in general to spin decoherence. A handle to adjust the impact of the action variable on the average revolution period, which can be used to decrease spin decoherence, is sextuples placed at positions with dispersion.

6 Conclusions

The study has led to several key findings about vertical spin build-up due to vertical offsets in magnetic and electric quadrupoles, in combination with horizontal betatron oscillations. For focusing with magnetic quadrupoles, the vertical spin build-up obtained in simulations is about half the one expected from derivations and of opposite sign. It is unclear whether additional not yet identified effects cause this discrepancy. The spin build-up rate is as expected proportional to the vertical quadruple offset and the horizontal action variable.

Instead very good agreement between analytical estimates and simulation results is observed for the case with focusing with electro-static quadrupoles.

Operation strategies involving counter-rotating beams and varying quadrupole polarities may mitigate systematic errors. However, residual effects due to different beam emittances for the two counter-rotating beams and imperfect magnetic field inversion need further investigation.

References

[1] Yannis K. Semertzidis. A new experiment for an electric dipole moment of muon at the 10^{-24}e $\cdot$ cm level. In *Proceedings of the Workshop on Frontier Tests of Quantum Electrodynamics and Physics of the Vacuum, Sandansky, Bulgaria*, 1998.

[2] I.B. Khriplovich. Feasibility of search for nuclear electric dipole moments at ion storage rings. *Physics Letters B*, 444(1-2):98–102, 1998.

[3] F.J.M. Farley, K. Jungmann, J.P. Miller, W.M. Morse, Yu F. Orlov, B.L. Roberts, Yannis K. Semertzidis, A. Silenko, and E.J. Stephenson. New method of measuring electric dipole moments in storage rings. *Physical review letters*, 93(5):052001, 2004.

[4] Y. Senichev, S. Andrianov, A. Ivanov, S. Chekmenev, M. Berz, and E. Valetov. Investigation of lattice for deuteron EDM ring. In *Proceedings of ICAP*, pages 17–19, 2015.

[5] Alexander Skawran and Andreas Lehrach. Spin tracking for a deuteron EDM storage ring. In *Journal of Physics: Conference Series*, volume 874, page 012050. IOP Publishing, 2017.

[6] A.E. Aksentev and Y.V. Senichev. Frequency domain method of the search for the electric dipole moment in a storage ring. In *Journal of Physics: Conference Series*, volume 1435, page 012047. IOP Publishing, 2020.

[7] V. Anastassopoulos, S. Andrianov, R. Baartman, S. Baessler, M. Bai, J. Benante, M. Berz, M. Blaskiewicz, T. Bowcock, K. Brown, et al. A storage ring experiment to detect a proton electric dipole moment. *Review of Scientific Instruments*, 87(11), 2016.

[8] Christian Carli and Malek Haj Tahar. Geometric phase effect study in electric dipole moment rings. *Phys. Rev. Accel. Beams*, 25:064001, June 2022.

[9] Zhanibek Omarov, Hooman Davoudiasl, Selcuk Hacıömeroğlu, Valeri Lebedev, William M. Morse, Yannis K. Semertzidis, Alexander J. Silenko, Edward J. Stephenson, and Riad Suleiman. Comprehensive symmetric-hybrid ring design for a proton EDM experiment at below 10^{-29}e $\cdot$ cm. *Phys. Rev. D*, 105:032001, Feb 2022.

[10] D.F. Nelson, A.A. Schupp, R.W. Pidd, and H.R. Crane. Search for an electric dipole moment of the electron. *Physical Review Letters*, 2(12):492, 1959.

[11] Takeshi Fukuyama and Alexander J. Silenko. Derivation of generalized Thomas-Bargmann-Michel-Telegdi equation for a particle with electric dipole moment. *International Journal of Modern Physics A*, 28(29):1350147, 2013.

[12] Bmad: Software toolkit for charged-particle and X-Ray simulations.

[13] Internal discussions with srEDM meetings.